# Moisture profiles determination during convective drying using X-ray microtomography

***ANGÉLIQUE LEONARD*, SILVIA BLACHER, PIERRE MARCHOT, JEAN-PAUL PIRARD, MICHEL CRINE***

***Laboratory of Chemical Engineering, Department of Applied Chemistry, University of Liège, Building B6c – Sart Tilman, 4000 Liège, Belgium***

The knowledge of internal moisture profiles which develop during drying is essential for model validation purposes, but they are difficult to determine experimentally. This paper shows that X-ray microtomography, together with image analysis, provides an accurate, non destructive and easy to use technique to determine moisture profiles. Results reported concern the drying of wastewater sludges whose management is becoming a real environmental challenge. An analysis of the development of moisture gradients at the sample external wall shows an influence of drying operating conditions. Finally, mass diffusion coefficients are estimated from the knowledge of both the moisture gradients and the drying flux.

La connaissance des profils d'humidité internes se développant durant le séchage est essentielle pour la validation de modèles de simulation, mais ils sont difficilement accessibles expérimentalement. La microtomographie à rayons X, couplée à l'analyse d'images, permet de les mesurer d'une manière précise, aisée et non destructive. Ceci est illustré dans le cas du séchage de boues d'épuration, dont la gestion va devenir cruciale. Une relation entre les conditions opératoires et le développement de gradients à la paroi est mise en évidence. La connaissance du flux de séchage et des gradients à la paroi permet une estimation du coefficient de diffusion interne.

* Author to whom correspondence should be addressed. E-mail address: A.Leonard@ulg.ac.be

Keywords: Moisture profiles, convective drying, X-ray microtomography, sludges, diffusion coefficient.

Drying is a highly energy consuming thermal treatment representing 10-15 % of the world industrial energy consumption (Kerkhof and Coumans, 2002). Actually, this operation also strongly affects the final quality and the textural properties of the dried material. The optimal control of a drying process is thus critical and needs a good understanding of the material drying behaviour. Comparison of actual and predicted moisture profiles which develop during drying gives a measure of kinetic models validity. However, the difficulty to obtain experimental measurements has limited the ability of drying models validation (Waananen et al., 1993). Up to now, moisture profiles have been mainly determined either by a destructive technique such as slicing (Couturier et al., 2000) or by a sophisticated non destructive method such as nuclear magnetic resonance (Ruan et al., 1991; Frias et al., 2002). To our knowledge this is the first time X-ray microtomography is used to measure moisture profiles during drying. In addition to its non destructive character, X-ray microtomography is a fast and easy to use technique. Most of the image analysis treatment can be easily automated once the data processing has been elaborated.

Results reported concern wastewater sludges. Sludge management and disposal is becoming a big challenge. It is now well established that a thermal drying operation, after dewatering, is an essential step before incineration or landspreading which constitute the two most relevant issues in the future, explaining the growing number of papers dedicated to sludge drying (Kazakura and Hasatani, 1996; Ferrasse et al., 2002; Vaxelaire and Puiggali, 2002; Léonard, 2003).

## Materials and methods

*Sample preparation*

Sludge samples (3-4 % dry matter.) are collected in a domestic wastewater treatment plant, after secondary settling and thickening. Sludge samples are flocculated in a bench scale jar-test by adding 0.006 kg/kg dry matter of a cationic polyelectrolyte (Zetag 7587 from Ciba). Dewatering is realized in a normalized filtration-expression cell (AFNOR, 1979) under a differential pressure of 304 kPa. The cake recovered after filtration (15 ± 2 % dry matter.) is extruded through a circular die of 12 mm diameter, producing cylindrical extrudates similar to those used in several industrial belt dryers. Extrudates are cut at a length of 15 mm, yielding samples with volume and mass of approximately 1.7 $cm^3$ and 2 g, respectively.

*Microdrying set-up*

Convective drying experiments are carried out in a so-called 'micro-drier' specially designed for handling small extruded samples with a mass between 0.5 and 5 g. The micro-drier is composed of two parts : the air conditioning system and the drying chamber. Air is fed from a laboratory compressed air network. Its flowrate is controlled by a pneumatic valve connected to a mass flowmeter. Air can be humidified by means of a steam generator, heated up to the required temperature by passing through a heating channel and then directed to the drying chamber. Air humidity, temperature and flowrate are continuously monitored and controlled. The sludge sample lies on a supporting grid linked underneath to a precision-weighing device. The sample surrounding is such that drying proceeds on the entire external sample surface. The weighing device is connected to a computer which allows the acquisition of mass versus time.

*X-ray microtomograph*

X-ray tomography is a non-invasive technique allowing the visualization of the internal texture of a material. During tomographic investigation, an X ray beam is sent on the sample and the

transmitted beam is recorded on a detector. According to Beer-Lambert law, the transmitted intensity is related to the integral of the X-ray attenuation coefficient μ along the path of the beam. This coefficient μ depends on the density ρ and the atomic number Z of the material, and on the energy of the incident beam E according to Equation (1) in which a is a quantity with a relatively small energy dependence, and b is a constant (Vinegar and Wellington, 1987). Projections (assembling of transmitted beams) are recorded for several angular positions by rotating the sample between 0 and 180°C. Then a back-projection algorithm is used to reconstruct 2D or 3D images, depending on the method used. In the case of 2D images, each pixel has a grey level value corresponding to the local attenuation coefficient.

$$\mu = \rho\left(a + \frac{bZ^{3.8}}{E^{3.2}}\right) \quad (1)$$

The X-ray microtomographic device used in this study is a "Skyscan-1074 X-ray scanner" (Skyscan, Belgium). Advanced technical details about its conception and operation are described by Sasov and Van Dyck (1998). The X-ray source operates at 40 kV and 1 mA. The detector is a 2D, 768×576 pixels, 8-bit X-ray camera with a spatial resolution of 41 μm. The following sequence is repeated several times during a drying experiment: drying interruption – tomographic analysis – drying resumption. Once the sample is placed in the microtomograph, a zone covering approximately a height of 1 cm is selected for tomographic investigation. The rotation step is fixed at 3.6 degree in order to reduce acquisition time down to 2 minutes. This is necessary to avoid relaxation of moisture profiles and further drying of the sample. A previous work has shown that repeated interruptions of the drying experiment have no significant effect on drying kinetics (Léonard et al., 2001). A classical back projection algorithm is used to reconstruct 2D images of the cross-sections. Two different methods were tested to correct beam hardening artefacts: an image post-processing method developed by the authors, and a pre-processing method available in a commercial reconstruction software (Wts.exe, Skyscan). The correction quality was evaluated by

comparing corrected grey level profiles at the beginning (completely wet) and at the end (completely dry) of a drying run, i.e., when these profiles should be flat. As differences between both correction methods appeared to be not significant, the second option was adopted because it was more convenient to use on a routine basis.

*Image analysis*

An original image analysis processing has been developed in order to perform a grey level analysis of the 2D images. The program has been implemented in Matlab software, with image analysis toolbox version 6.0 from Matworks. For each cross-section, the mean grey level intensity is determined in concentric rings of a grid defined as the successive boundaries of each cross-section eroded several times, depending of the initial section diameter. This construction allows to take into account the particular geometry of each cross-section. Figures 1A and 1B show the two grids obtained for a cross section of the same sample respectively before and after drying. Each ring has a thickness of 5 pixels or 0.205 mm. Figure 1B also indicates some cracks develop during the drying operation. In each ring, the so-called 'crack ratio' (area of cracks divided by the total cross section area) is determined from binarised images in order to calculate the grey level characteristic of the mixture water+dry matter.

Figure 2 shows some grey level profiles obtained at increasing drying times corresponding to decreasing water contents W expressed on a dry basis. Grey levels appearing on this figure are averaged on the different cross-sections, in a same ring. The x-axis represents the radial distance between the external wall of the sample (x=0) and the considered ring, up to the centre of the sample. These curves have been obtained during a convective drying experiment at a constant temperature of 120 °C, with air at ambient humidity without any vapour addition (absolute humidity ~ 0.006 kg/kg dry air) and a superficial velocity of 1 m/s. Decreasing distances between the wall

and the centre of sample illustrate the shrinkage observed during drying. As drying proceeds, the mean grey level of the cross-sections increases, indicating an increase of the mean X-ray attenuation coefficient of the investigated material. This reflects that the dry matter of the sludge is more absorbent than water.

At the pixel level, it is not possible to discriminate between water or part of the solid skeleton. We consider that each pixel has a grey level value corresponding to an average between dry solid and pure water contributions (Equation (3)). After rearrangement we obtain Equation (4), showing a theoretical linear relation between water content (expressed on a wet basis and comprised between 0 and 1) and the grey level of the wet solid, measured by microtomography.

$$(\text{Grey level})_{\text{Wet Solid}} = \text{Water content } (\text{Grey level})_{\text{Water}} + (1\text{-Water content}) (\text{Grey level})_{\text{Dry Solid}} \quad (3)$$

$$\text{Water content} = \frac{(\text{Grey level})_{\text{Dry Solid}} - (\text{Grey level})_{\text{Wet Solid}}}{(\text{Grey level})_{\text{Dry Solid}} - (\text{Grey level})_{\text{Water}}} \quad (4)$$

Figure 3 shows the calibration curve obtained by plotting, for each drying interruption, the mean water content (on a wet basis) of the whole sample versus the mean grey level (cracks excepted) of the 2D reconstructed images. All these points correspond to 27 drying experiments according to a complete $3^3$ factorial design described in Table 1. As expected, a linear relation has been found, indicating the good reliability of the tomographic measurements. Nevertheless, the accuracy of the results is clearly better at high water content, before the development of large cracks, i.e., at water content larger than 30 %. At lower water content, experimental data are more scattered mainly because of the sample heterogeneity at the end of drying. The calibration curve gives also some indications on the reproducibility on the method. Indeed, before drying the 27 samples have approx. the same water content, i.e. 85%, for a same corresponding grey level close to 35.

## Results

Figure 4 shows the moisture profiles calculated from the grey level profiles of Figure 2, using the calibration curve represented on Figure 3. At the beginning of drying, i.e. at high water content, the local moisture content remains uniformly distributed throughout the sample indicating high mass transfer inside the sludge sample. As drying proceeds, some gradients appear at the wall resulting from internal mass transfer limitations. Moisture gradients at the external sample wall are determined by fitting and derivating a quadratic curve on the 5-6 points situated closest the wall (Figure 5). Figure 6 shows the evolution of wall moisture gradients during the course of drying for two sets of operating conditions differing only by the absolute humidity of air. A normalized water content $W/W_0$ is used as abscissa in order to account for small differences between initial water contents ($W_0$) of each sample. It can be observed that the development of the moisture gradient is delayed when increasing air humidity. The same behaviour is observed when decreasing air superficial velocities are employed (Figure 7), at a higher temperature. These observations may be related to the effect of velocity and humidity on the mass transfer Biot number. Increasing humidities and decreasing velocities lower the Biot number what corresponds to a reduction of internal transfer limitations versus external transfer limitations (Liu et al., 1997).

### *Diffusion coefficient determination*

Diffusion coefficients are estimated from moisture gradients and mass flux (Equation (5)) at the external wall. The mass flux is determined from drying rate and shrinkage curves. Measurement of shrinkage is performed by X-ray microtomography as explained elsewhere (Léonard et al., 2002). In this equation a moisture mass concentration C is needed, instead of moisture percentage as used in Figure 4. The transformation of one to another type of unit is easily achieved as the volume and the mass of the sample are known throughout the drying process. The diffusion coefficient obtained ranges from $10^{-11}$ to $7\ 10^{-10}$ m²/s, which agrees fairly well with data reported in the literature for

sludges and some other materials (see Table 2). This is an indication of the good accuracy of the method, which should be confirmed by comparison with value obtained through simulation models of the drying kinetics.

$$F = -D\left.\frac{dC}{dx}\right|_{x=0} \qquad (5)$$

Figure 8 shows the evolution of the diffusion coefficient versus sample water content. All these data correspond to the 27 experiments described in Table 1. As commonly observed, the diffusion coefficient decreases with water content, inducing increasing internal transfer limitations during the course of the drying process. No effect of the temperature has been detected. Different laws (power law, exponential, polynomial,…) are used in the literature in order to model the dependence of the diffusion coefficient versus the water content (Mujumdar, 1995). In our case, an exponential law (Equation (6)) has been chosen. Table 3 gives the results obtained after linear fitting of Equation (6) in its logarithmic form.

$$D = A\exp(BW) \qquad (6)$$

## Conclusions

X-ray microtomography, associated to image analysis, is a fast and easy to use non destructive technique. X-ray microtomography is a useful tool to measure moistures profiles which develop during convective drying of wastewater sludge. Most of the image analysis treatment can be easily automated once the data processing has been elaborated. An analysis of the moisture gradients development under different operating conditions confirms gradients are smoother and appear later if air humidity increases or if air temperature decreases. From the knowledge of moisture gradients and mass drying flux, the diffusion coefficients are estimated at different sample water contents.

Values obtained are in agreement with those mentioned in the literature. The dependence of the diffusion coefficient with water content can be modeled by an exponential law. All these information provided by X-ray microtomography are of crucial need in the field of drying modeling and drying optimization. In the continuation of this work, a study is currently carried out in order to investigate relations between moisture gradients and the evolution of the sludge texture (shrinkage, crack development) during drying. Furthermore, we are working on the development of a fully coupled thermo-hydro-mechanical model which will allow the comparison between predicted and measured internal moisture profiles.

## Acknowledgements

A. Léonard is grateful to the FNRS (National Fund for Scientific Research, Belgium) for a Scientific Research Worker position. The authors thank the FNRS, the Ministère de la Région Wallonne (DGTRE), the Ministère de la Communauté française-Direction de la Recherche scientifique (ARC 00/05-265) and the Fonds de Bay (University of Liège) for their financial support.

## Nomenclature

A = Fitting parameter (Equation 6)

B = Fitting parameter (Equation 6)

C = Volume concentration ($kg/m^3$)

E = X-ray beam energy (V)

F = Mass drying flux ($kg/m^2.s$)

D = Diffusion coefficient ($m^2/s$)

W = Water content on a dry basis (kg/kg)

$W_0$ = Initial water content on a dry basis (kg/kg)

x = Distance between the external wall and the center of the sample (m)

Z = Atomic number (-)

*Greek letters*

$\alpha$ = Confidence coefficient (-)

$\rho$ = Density ($kg/m^3$)

## References

AFNOR, "Tests on sludges - Determination of properties related to thickening capacity", AFNOR T 97-001, (1979).

Andrieu, J. and Stamatopoulos, A., "Durum wheat pasta drying kinetics", Lebensm-Wiss Technol. **19**, 448-456 (1986).

Couturier, S., J. Vaxelaire, and J. R. Puiggali, "Convective drying of domestic activated sludge", in "Proceedings of the 12th International Drying Symposium, Noordwijkerhout, The Netherlands, Aug 28-31, 2000″,P. J. A. M. Kerkhof, W. J. Coumans, and G. D. Mooiweer, Eds., (2000), Paper 44.

Ferrasse, J.-H., Arlabosse, P. and Lecomte, D., "Heat, momentum, and mass transfer measurements in indirect agitated sludge dryer", Dry. Technol. **20**, 749-769 (2002).

Frias, J. M., Foucat, L., Bimbenet, J. J. and Bonazzi, C., "Modeling of moisture profiles in paddy rice during drying mapped with magnetic resonance imaging", Chem. Eng. J. **86**, 173-178 (2002).

Hills, B. P., Godward, J. and Wright, K. M., "Fast Radial NMR Microimaging Studies of Pasta Drying", J. Food Eng. **33**, 321-335 (1997).

Kazakura, T. and Hasatani, M., "R&D needs - Drying of sludges", Dry. Technol. **14**, 1389-1401 (1996).

Kerkhof, P. J. A. M. and Coumans, W. J., "Drying: a fascinating unit operation", Chem. Eng. J. **86**, 1-2 (2002).

Kim, J.-K. and Lee, C.-S., "Prediction of differential drying shrinkage in concrete", Cement Concrete Res. **28**, 985-994 (1998).

Léonard, A., "Etude du séchage convectif de boues de station d'épuration - Suivi de la texture par microtomographie à rayons X", PhD Thesis, Université de Liège, Belgique (2003).

Léonard, A., S. Blacher, P. Marchot, and M. Crine, "X-ray microtomography : a new tool to follow soft material shrinkage during convective drying", in "Proceedings of the Second World Congress on Industrial Process Tomography, Hanover, Germany, Aug 29-31, 2001″(2001), pp.110-117.

Léonard, A., Blacher, S., Marchot, P. and Crine, M., "Use of X-ray microtomography to follow the convective heat drying of wastewater sludges", Dry. Technol. **20**, 1053-1069 (2002).

Liu, H., Zhou, L. and Hayakawa, K. I., "Sensitivity analysis for hygrostress crack formation in cylindrical food during drying", J. Food Sci. **62**, 447-450 (1997).

Mujumdar, A. S., "Handbook of industrial drying", A. S. Mujumdar, Ed., Marcel Dekker, New York (1995).

Queiroz, M. R. and Nebra, S. A., "Theoretical and experimental analysis of the drying kinetics of bananas", J. Food Eng. **47**, 127-132 (2001).

Ruan, R., Schmidt, S. J., Schmidt, A. R. and Litchfield, J. B., "Non-destructive measurement of transient moisture profiles and moisture diffusion coefficient in a potato during drying and absorption by NMR imaging", J. Food Process Eng. **14**, 297-313 (1991).

Saravacos, G. D. and Charm, S. E., "A study of the mechanism of fruit and vegetable dehydration", J. Food Technol., 78-81 (1962).

Sasov, A. and Van Dyck, D., "Desktop X-ray microscopy and microtomography", J. Microsc. **191**, 151-158 (1998).

Vaxelaire, J. and Puiggali, J. R., "Analysis of the drying of residual sludge: from the experiment to the simulation of a belt dryer", Dry. Technol. **20**, 989-1008 (2002).

Vinegar, H. J. and Wellington, S. L., "Tomographic imaging of three-phase flow experiments", Rev. Sci. Instrum. **58**, 96-107 (1987).

Waananen, K. M., Litchfield, J. B. and Okos, M. R., "Classification of drying models for porous solids", Dry. Technol. **11**, 1-40 (1993).

Table 1 : 3×3 factorial design

| | Level 1 | Level 2 | Level 3 |
|---|---|---|---|
| Temperature (°C) | 80 | 120 | 160 |
| Superficial velocity (m/s) | 1 | 2 | 3 |
| Air humidity (kg/kg) | 0.006 | 0.15 | 0.41 |

Table 2 : Diffusion coefficients for different kind of materials

| Material | D ($m^2/s$) | $W_0$ (kg/kg) | Authors |
|---|---|---|---|
| Wastewater sludge | $0.5\ 10^{-10}$ to $9\ 10^{-10}$ | 4.5 | (Couturier et al., 2000) |
| Potatoes | $2.58\ 10^{-10}$ to $6.36\ 10^{-10}$ | 5 | (Saravacos and Charm, 1962) |
| Pasta | $0.08\ 10^{-10}$ to $0.9\ 10^{-10}$ | 0.42 to 0.50 | (Andrieu and Stamatopoulos, 1986) |
| Pasta | $5.2\ 10^{-10}$ | 0.68 | (Hills et al., 1997) |
| Concrete | $5\ 10^{-10}$ | 0.09 | (Kim and Lee, 1998) |
| Banana | $1.25\ 10^{-10}$ to $6.98\ 10^{-10}$ | 4.5 | (Queiroz and Nebra, 2001) |
| Rice | $0.00368\ 10^{-10}$ | 0.25 | (Frias et al., 2002) |

Table 3 : Results of the linear fitting of Equation 2

| | Parameter | Confidence Limits ($\alpha = 0.95$) |
|---|---|---|
| A | $1.8\ 10^{-11}$ | $4\ 10^{-12}$ |
| B | 0.75 | 0.10 |

Figure captions

Figure 1 : Grids obtained to measure grey level in a cross section a) before and b) after drying

Figure 2 : Grey level profiles obtained at different residual water contents

Figure 3 : Calibration curve : sample water content versus image grey level

Figure 4 : Moisture profiles at different residual water contents

Figure 5 : Fit of a quadratic curve to determine moisture gradients at the wall of the sample

Figure 6 : Influence of air absolute humidity on gradients development

Figure 7 : Influence of air superficial velocity on gradients development

Figure 8 : Diffusion coefficient versus water content

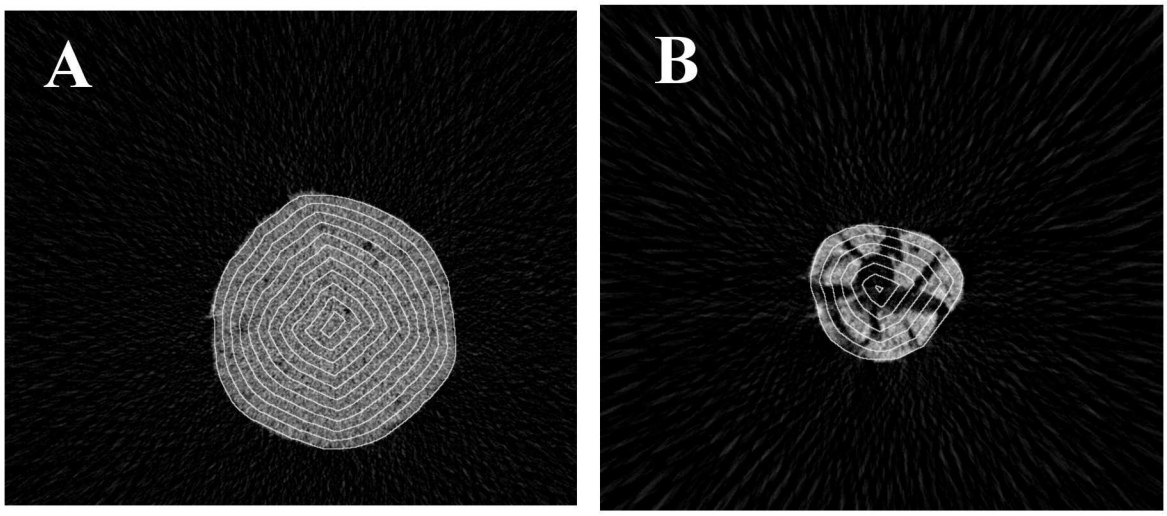


Figure 1 : Grids obtained to measure grey level in a cross section a) before and b) after drying

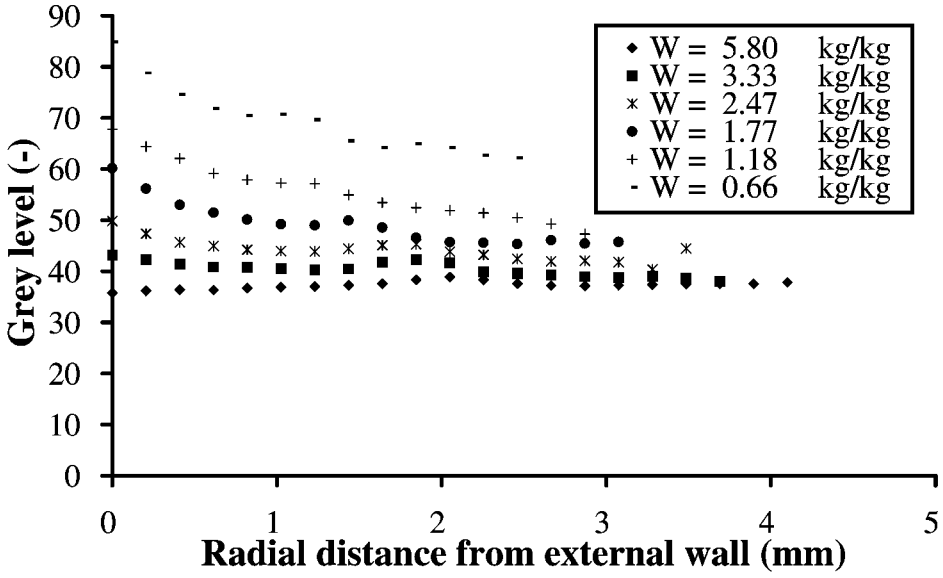


Figure 2 : Grey level profiles obtained at different residual water contents

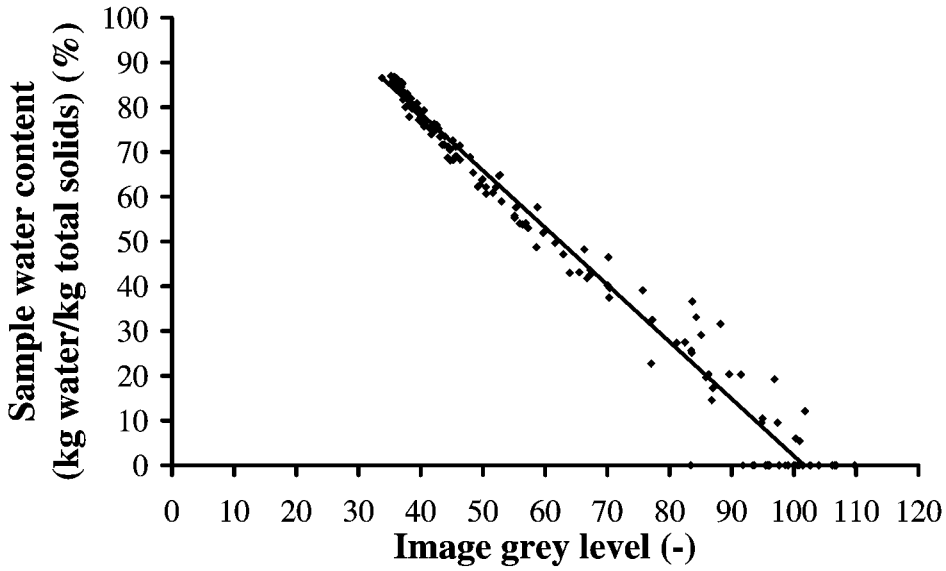


Figure 3 : Calibration curve : sample water content versus image grey level

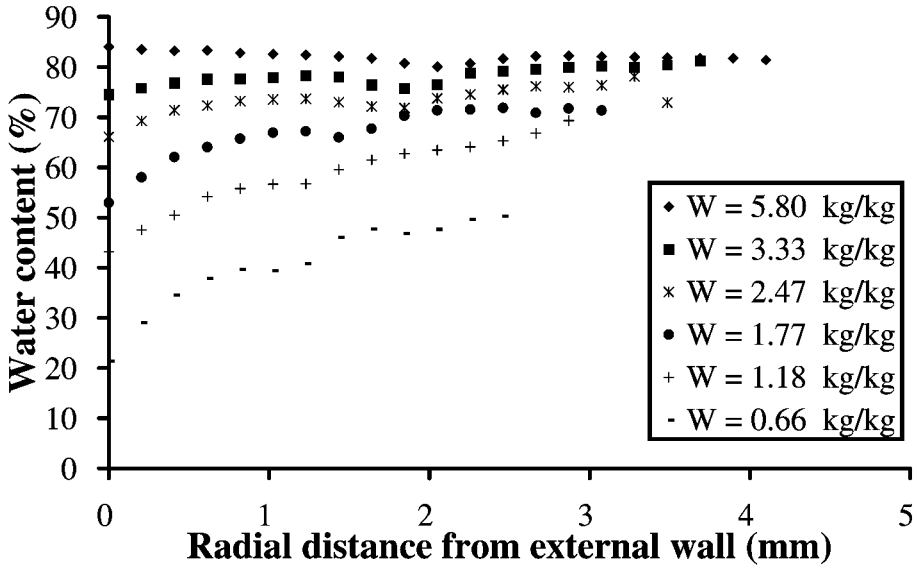


Figure 4 : Moisture profiles at different residual water contents

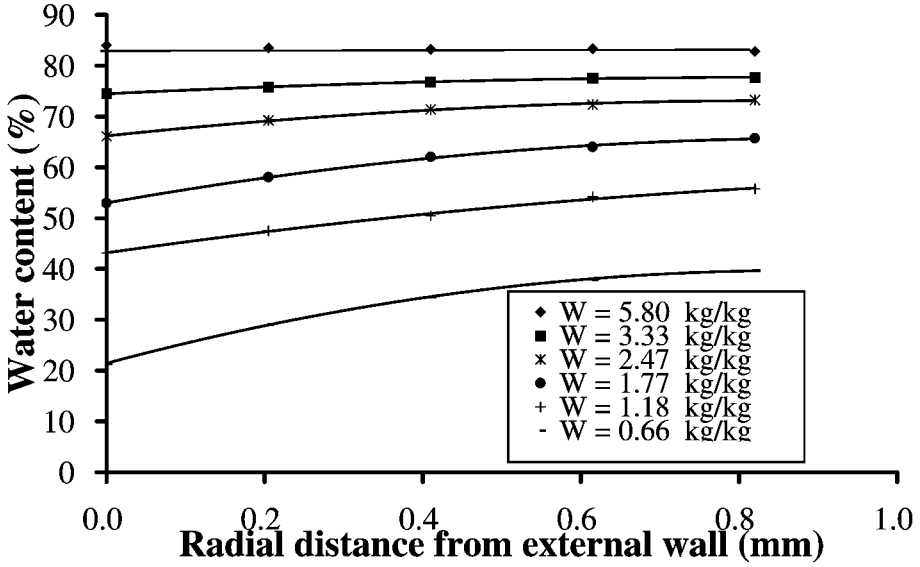


Figure 5 : Fit of a quadratic curve to determine moisture gradients at the wall of the sample

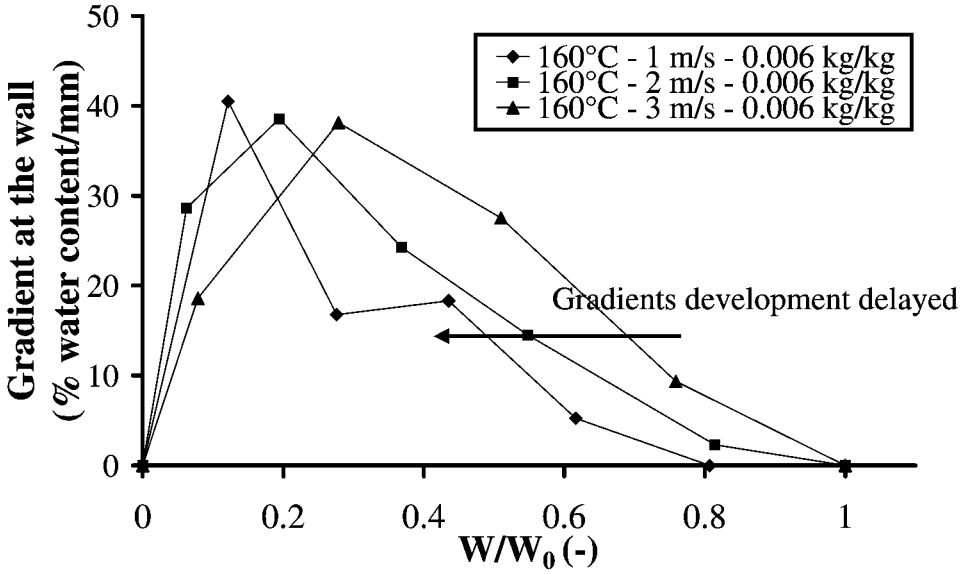


Figure 6 : Influence of air absolute humidity on gradients development

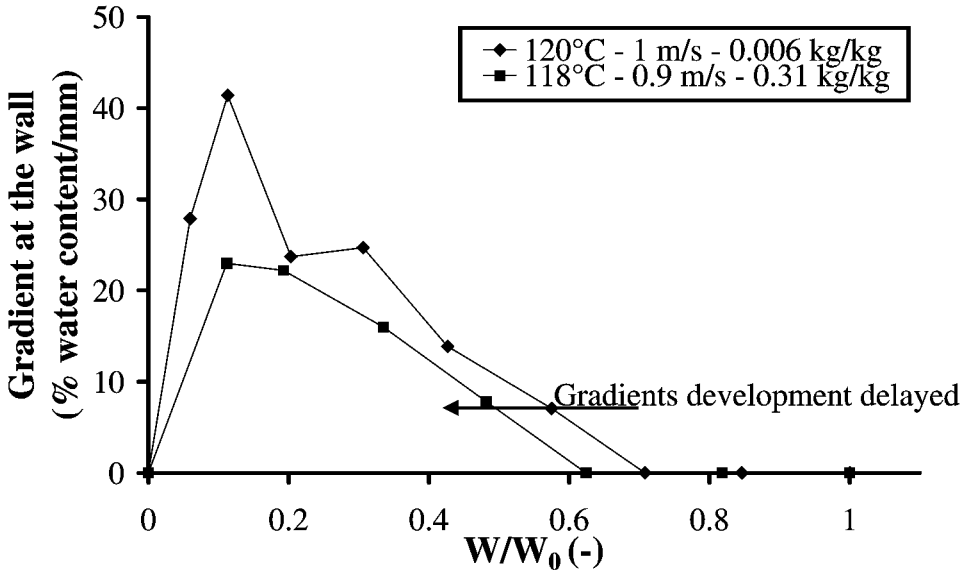


Figure 7 : Influence of air superficial velocity on gradients development.

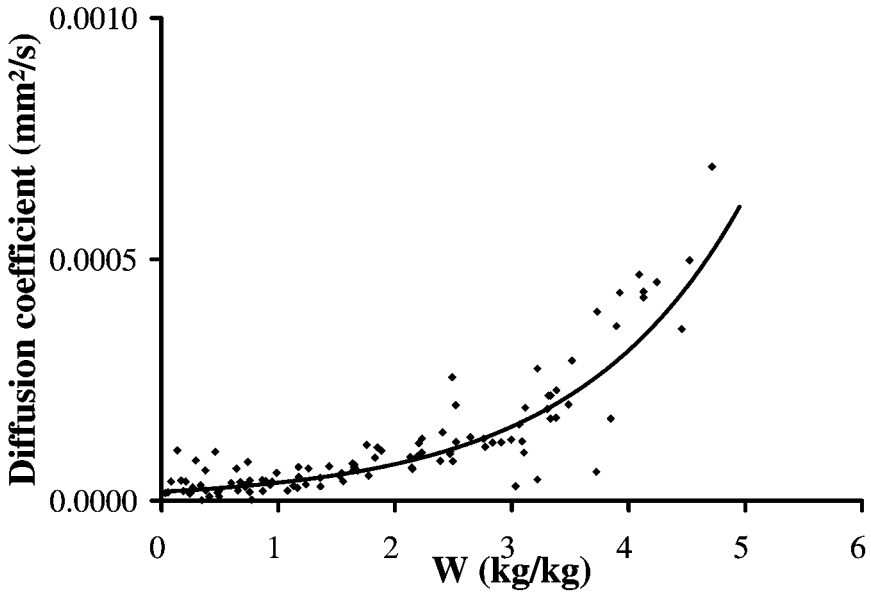


Figure 8 : Diffusion coefficient versus water content